Inorganic Chemistry

Communication

pubs.acs.org/IC

Polymeric Perturbation to the Magnetic Relaxations of the C_{2v}-Symmetric $[Er(Cp)_2(OBu)_2]^-$ Anion

Tian Han,[†] You-Song Ding,[†] Ji-Dong Leng,[†] Zhiping Zheng,[†,‡] and Yan-Zhen Zheng*,[†]

[†]Center for Applied Chemical Research, Frontier Institute of Science and Technology, and MOE Key Laboratory for Nonequilibrium Synthesis and Modulation of Condensed Matter, Xi'an Jiaotong University, Xi'an 710054, China

[‡]Department of Chemistry and Biochemistry, University of Arizona, Tucson, Arizona 85721, United States

Supporting Information

ABSTRACT: To test the coordination symmetry effect on the magnetization-reversal barrier trend of Er^{III}-based single-ion magnets, the C_{2v}-symmetric organolanthanide anion $[Er(Cp)_2(O^tBu)_2]^-$ has been incorporated with different countercations, resulting in two structures, namely, the discrete $[K_2(Cp)(18\text{-}C\text{-}6)_2][Er(Cp)_2(O^tBu)_2]$ (**1**) and the polymeric $[ErK_2(Cp)_3(O^tBu)_2(THF)_2]_n$ (**2**), where 18-C-6 = 18-crown-6 ether and Cp = cyclopentadienide. Surprisingly, the polymeric **2** exhibits much stronger field-induced magnetization relaxing behavior compared to the monomeric **1**. Such disparate dynamic magnetism is attributable to the subtle coordination environmental perturbations of the central Er^{III} ions.

Lanthanide-based single-ion magnets (SIMs), characterized by the presence of 4f ions with large unquenched orbital moments and significant magnetic anisotropies, are promising candidates for size-reduced information storage devices.[1] Considerable effort has been devoted to enhancing the energy barrier to reversal of magnetization in lanthanide SIMs in order to achieve high blocking temperatures.[2,3] Notable examples include the highest relaxation energy barrier (938 K) in a mononuclear terbium(III) compound[2c] and the second highest barrier (842 K) in a multinuclear dysprosium(III) cluster,[4] from which the magnetic anisotropy of single lanthanide ions has been highlighted.

It is generally accepted that the axial symmetry of a crystal field with a single high-order rotation axis, C_n ($n > 2$), around the lanthanide ion can effectively reduce the probability of quantum tunneling processes that shortcut the thermal energy barrier.[1] However, this may be only true for an oblate ion, such as the Dy^{III} ion.[5−7] For a prolate ion such as Er^{III}, an equatorial ligand field, and therefore high-symmetry coordination in the equatorial plane, is required.[3,5,8] This constraint of the equatorial symmetry seems more challenging because coordination deviating out of the equatorial plane is easier for the lanthanide ions, whose coordination is primarily ionic in nature and therefore dynamic, determined mostly by the energy minimization of the coordination sterics.

This high proneness to structural distortion may be responsible for the small number of Er^{III}-containing SIMs in the literature.[3] So far, nearly all of the reported Er^{III}-based SIMs adopt high-symmetry coordination, including D_{8d}, $C_{\infty v}$, D_{4d}, and C_{3v}.[3] Moreover, the energy barriers for magnetization reversal in these Er^{III}-based SIMs roughly show a trend of descent with decreasing local coordination symmetry (see also the discussion below). Thus, to further test such a hypothesis, filling in the blanks of other symmetries such as C_{2v} seems necessary.

Herein, we report a unique pair of erbium(III) compounds, one discrete, $[K_2(Cp)(18\text{-}C\text{-}6)_2][Er(Cp)_2(O^tBu)_2]$ (**1**; 18-C-6 = 18-crown-6 ether, Cp = cyclopentadienide, and O^tBu = *tert*-butoxide), and the other polymeric, $[ErK_2(Cp)_3(O^tBu)_2(THF)_2]_n$ (**2**; THF = tetrahydrofuran). Despite the fact that they share a common anionic unit of $[Er(Cp)_2(O^tBu)_2]^-$ with C_{2v} symmetry, these two compounds display rather diverse dynamics of field-induced magnetic relaxation behavior. Structural analysis reveals that such disparity may be a result of subtle coordination environmental perturbations of the central Er^{III} ions when incorporated with different neighboring cations.

Essentially started from the ligand Cp,[9] compounds **1** and **2** were prepared according to Scheme 1 by treating $[ErCp_3]$ or $[ErCp_2Cl]$[10] with ^{t}BuOK in the presence of 18-C-6 in THF for **1** or using $[ErCp_2Cl]$ in THF for **2**.

Scheme 1. Syntheses of 1 and 2

$$[ErCp_3] \text{ or } [ErCp_2Cl] + 2t\text{-BuOK} \xrightarrow[\text{THF}]{\text{18-C-6}} [K_2(Cp)(18\text{-}C\text{-}6)_2][Er(Cp)_2(O^tBu)_2] \quad (1)$$

$$[ErCp_2Cl] + 2t\text{-BuOK} \xrightarrow[\text{THF}]{} [ErK_2(Cp)_3(O^tBu)_2(THF)_2]_n \quad (2)$$

Single-crystal X-ray analysis of **1** reveals that the Er^{III} center is octacoordinate with two η^5-Cp ligands and two O^tBu O atoms, resulting in local C_{2v} symmetry (Figure 1a,b and Figure S1 and Tables S1 and S2 in the Supporting Information, SI). A countercation of $[K_2(Cp)(18\text{-}C\text{-}6)_2]^+$ sits next to the $[Er(Cp)_2(OBu)_2]^-$ anion. With the shortest Er···Er separation of 9.21 Å, the anionic complex unit is essentially isolated (Figure S2 in the SI).

The Er^{3+} ion of **2** is also coordinated by two η^5-Cp ligands and two O^tBu O atoms (Figures 1c,d and Figure S3 and Tables S3 and S4 in the SI). However, both ligands are bridging, resulting in a slight change of the Er−C (2.690−2.745 Å with an average of 2.720 Å versus a range of 2.696−2.769 Å with an average of 2.738 Å for **1**) and Er−O (2.069 Å for **1** and 2.101 Å for **2**) bond lengths. We note that the difference in the O−Er−O bond angles is much more profound (102.0° for **1** and 92.8° for **2**), and so are

Received: January 28, 2015
Published: April 30, 2015

DOI: 10.1021/acs.inorgchem.5b00213
Inorg. Chem. 2015, 54, 4588−4590

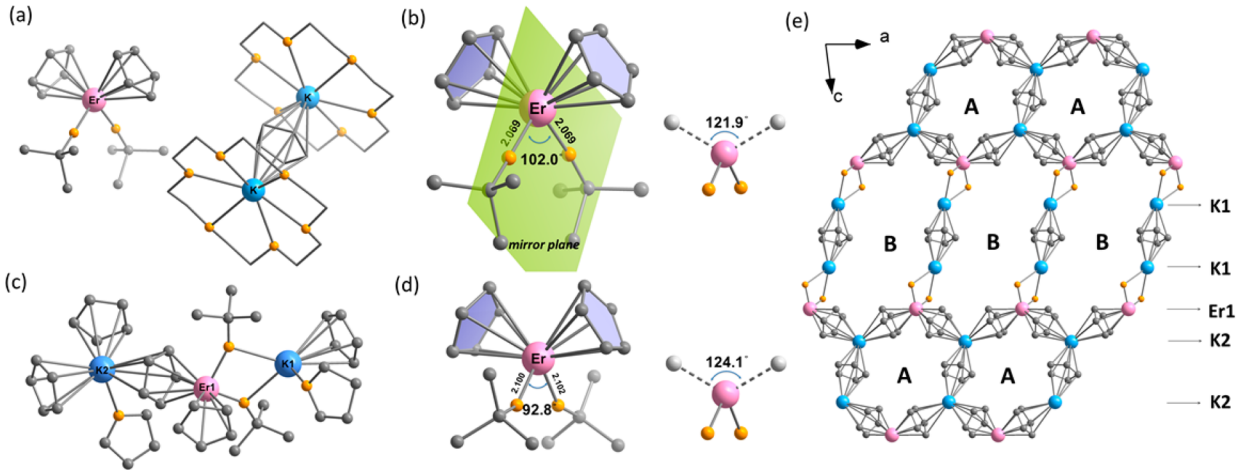

Figure 1. (a) Molecular structure of **1**. (b) $[Er(Cp)_2(OBu)_2]^-$ anion and its pseudotetrahedral geometry in **1**. (c) Molecular structure of **2**. (d) $[Er(Cp)_2(OBu)_2]^-$ anion and its pseudotetrahedral geometry in **2**. (e) 2D network of **2** as viewed along the *b* axis. Disorder of Cp rings, THF molecules, C atoms on *tert*-butoxide anions, and H atoms are omitted for clarity. Color code: pink, Er; orange, O; blue, K; gray, C.

the $Cp_{central}\cdots Er\cdots Cp_{central}$ angles (121.9° for **1** and 124.1° for **2**). Considering the tetrahedron defined by two O atoms of the O^{t}Bu groups and two Cp centroids, the Er^{III} coordination geometry in **1** is closer to an ideal tetrahedron than that in **2** calculated by the continuous symmetry measurement (CSM) method[11] (for **1**, 1.570; for **2**, 2.070).

Interestingly, in the polymeric structure of **2**, the Er1 and K2 atoms alternate and are linked by bridging Cp rings to form a heterometallic Er_2K_4 six-membered macrocycle with about 10.8 Å diameter (defined by the separation between the two diagonal Er^{3+}/K^+ atoms), marked as "A". Er1, K1, and K2 atoms are connected via Cp and O^{t}Bu bridges to form a decanuclear heterometallic Er_4K_6 rectangle (approximately 9.3 × 17.8 Å^2), denoted as "B". The "A" and "B" structures as building blocks are assembled to ladder chain "A" and "B" running parallel in the *a*-axial direction, which are alternating along the *c*-axial direction in an ABAB fashion (Figure 1e). The resulting 2D layers with the shortest Er···Er distance of 9.35 Å further stack via van der Waals interactions into a 3D molecular architecture (Figure S4 in the SI).

Direct-current (dc) magnetic susceptibility data were collected for **1** and **2** over the temperature range of 2−300 K (Figures S5 and S6 in the SI). At 300 K, the $\chi_M T$ products are 11.27 and 11.13 cm^3 K mol^{-1} for **1** and **2**, respectively, in good agreement with the calculated value for the Er^{III} ion (11.48 cm^3 K mol^{-1} for the $^4I_{15/2}$ state). Upon cooling, the $\chi_M T$ products decrease gradually at first and then more rapidly below 50 K, reaching minima of 5.10 and 6.86 cm^3 K mol^{-1} at 2 K for **1** and **2**, respectively. The magnetization at 2 K for both compounds shows a continuous increase with increasing field and unsaturated moments at 70 kOe (for **1**, 3.74 μ_B; for **2**, 4.66 μ_B). These behaviors, as well as the nonsuperimposition on the *M* versus HT^{-1} plots, are attributable to the presence of large magnetic anisotropy (Figures S7−S10 in the SI).

To gain insight into the dynamics of magnetization, alternating-current (ac) susceptibility measurements were performed. At zero dc field, no out-of-phase component (χ'') of the ac signal is observed for **1** or **2** (Figures S11 and S12 in the SI), whereas under an applied dc field, these two compounds exhibit rather different magnetization dynamics. Specifically, only slightly splitted χ'' is observed for **1**, while for **2**, a strong frequency-dependent out-of-phase susceptibility signal appears below 5 K, an indication of slow relaxation of magnetization (Figures 2 and S13 in the SI). Variable-frequency ac susceptibility

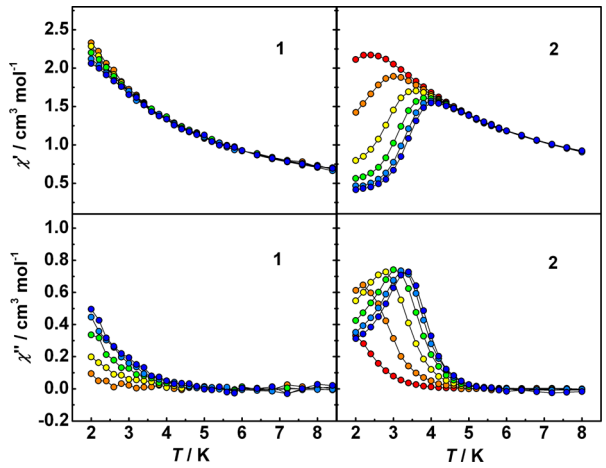

Figure 2. Temperature dependence of the in-phase (top) and out-of-phase (bottom) ac susceptibility for **1** and **2** in the range of 10 Hz (red) to 1500 Hz (blue) under an applied dc field (1.0 kOe for **1** and 1.5 kOe for **2**).

data for **2** at 2 K at a number of applied dc fields reveal two independent relaxation domains, one at high frequencies (10−1500 Hz, referred to as relaxation domain A) and the other at lower frequencies (0.1−10 Hz, referred to as relaxation domain B) (Figures S14−S16 in the SI). Relaxation times (τ) can be extracted by using the sum of two modified Debye functions.[12] The optimized dc field is estimated at 1.5 kOe, under which relaxation domains A and B are both well-defined. Additional ac measurements as a function of the frequency at 1.5 kOe with varying temperatures confirm such relaxations (Figures S17−S19 in the SI). Relaxation domain A shows semicircle Cole−Cole plots in the range of 2.0−3.8 K (Table S5 in the SI). At high temperatures, the relaxation time follows the Arrhenius law with a preexponential factor of $\tau_0 = 2.0 \times 10^{-8}$ s and an effective energy barrier of $U_{eff} = 28.5$ K, indicative of a thermally activated process. The data obtained at lower temperatures deviate from linearity in the Arrhenius plot. As such, the fast relaxation in domain A is likely ascribed to single-molecule-based magnetic

DOI: 10.1021/acs.inorgchem.5b00213
Inorg. Chem. 2015, 54, 4588−4590

relaxation. Relaxation domain B does not show any temperature dependence, with its relaxation time being 3 orders of magnitude slower than that of domain A; a linear increase in the relaxation time with an applied field and no asymmetry in Cole−Cole plots are observed. Such slow relaxation likely originates from an intermolecular relaxation pathway.[13]

With only C_{2v} symmetry in the $[Er(Cp)_2(OBu)_2]^-$ anion, the observed field-induced slow relaxation of magnetization in **2** suggests that the Er^{III} ion is adequately anisotropic but with a significant transverse feature, leading to SIM behavior only when quantum tunneling of the magnetization is effectively suppressed. A comparison with the previously reported Er^{III} SIMs (Table 1) reveals that the magnetic performance degrades roughly as the symmetry at the metal ion is lowered, from the observation of an open hysteresis loop up to 10 K in D_{8d} to a barrier of 323 K in $C_{\infty v}$, 122 K in C_{3v}, 55.2 K in D_{4d} in the absence of a dc field, 28.5 K in the present case, and 8.1 K in C_2 under an external field. It is possible that high symmetry favors collinearity of the principal magnetization axes for all of the Kramers doublets, leading to a large U_{eff} value.[14] In contrast, the absence of SIM behavior in **1** indicates that relaxation of the magnetization is sensitive to changes of the bond angles about the Er^{III} ion; such a change leads to further deviation of the Er^{III} coordination geometry from the pseudotetrahedral coordination geometry, which favors a stronger equatorial component. Thus, considering the magnetostructural correlation, the symbols $M^0U^0S^0$ and $M^0U^0S^2$ are appropriate to describe **1** and **2**, respectively.[15]

Table 1. Magnetization-Reversal Barriers for Er^{III}-Based SIMs

complex	local symmetry	U_{eff}/K	H_{dc}/kOe	ref
$[Er(COT)_2]^-$	D_{8d}	212	0	3d
ErCp*(COT)[a]	$C_{\infty v}$	197/323	0	3b
$Er[N(SiMe_3)_2]_3$	C_{3v}	122	0	3e
$[ErW_{10}O_{36}]^{9-}$	D_{4d}	55.2	0	3a
$[Er(Cp)_2(OBu)_2]^-$	C_{2v}	28.5	1.5	this work
$Er^{III}Zn^{II}_3$	C_2	8.1	1.0	3c

[a]ErCp*(COT) should be regarded with caution because one of the thermal processes does not fit the trend, and the local symmetry of Er^{III} is approximated to be $C_{\infty v}$ even with different rings and a bent geometry.

In summary, we have successfully incorporated the C_{2v}-symmetric $[Er(Cp)_2(OBu)_2]^-$ anions into both discrete and polymeric structures. Although the overall barriers for magnetization reversal in these two Er^{III}-based compounds are not high, they show interesting structure-perturbed magnetic relaxation behaviors. The more distorted tetrahedral coordination geometry of the Er^{III} ions is believed to be responsible for the enhanced field-induced SIM behavior observed in the polymeric compound.

■ ASSOCIATED CONTENT

Supporting Information

Experimental details, crystal and refinement details, additional magnetic data. The Supporting Information is available free of charge on the ACS Publications website at DOI: 10.1021/acs.inorgchem.5b00213.

■ AUTHOR INFORMATION

Corresponding Author

*E-mail: zheng.yanzhen@mail.xjtu.edu.cn.

Notes

The authors declare no competing financial interest.

■ ACKNOWLEDGMENTS

This work was supported by Grants 21201137, 2012CB619401, 21473129, and IRT13034, the China Postdoctoral Science Foundation (Grant 2014M552425), the "National 1000-Plan" program, and the Fundamental Research Funds for the Central Universities.

■ REFERENCES

(1) (a) Sessoli, R.; Powell, A. K. *Coord. Chem. Rev.* **2009**, *253*, 2328−2341. (b) Sorace, L.; Benelli, C.; Gatteschi, D. *Chem. Soc. Rev.* **2011**, *40*, 3092−3104. (c) Woodruff, D. N.; Winpenny, R. E. P.; Layfield, R. A. *Chem. Rev.* **2013**, *113*, 5110−5148. (d) Layfield, R. A. *Organometallics* **2014**, *33*, 1084−1099.

(2) (a) Ishikawa, N.; Sugita, M.; Ishikawa, T.; Koshihara, S. Y.; Kaizu, Y. *J. Am. Chem. Soc.* **2003**, *125*, 8694−8695. (b) Jiang, S. D.; Wang, B. W.; Su, G.; Wang, Z. M.; Gao, S. *Angew. Chem., Int. Ed.* **2010**, *49*, 7448−7451. (c) Ganivet, C. R.; Ballesteros, B.; de la Torre, G.; Clemente-Juan, J. M.; Coronado, E.; Torres, T. *Chem.—Eur. J.* **2013**, *19*, 1457−1465.

(3) (a) Aldamen, M. A.; Clementa-Juan, J. M.; Coronado, E.; Martí-Gastaldo, C.; Gaita-Ariño, A. *J. Am. Chem. Soc.* **2008**, *130*, 8874−8875. (b) Jiang, S. D.; Wang, B. W.; Sun, H. L.; Wang, Z. M.; Gao, S. *J. Am. Chem. Soc.* **2011**, *133*, 4730−4733. (c) Yamashita, A.; Watanabe, A.; Akine, S.; Nabeshima, T.; Nakano, M.; Yamamura, T.; Kajiwara, T. *Angew. Chem., Int. Ed.* **2011**, *50*, 4016−4019. (d) Meihaus, K. R.; Long, J. R. *J. Am. Chem. Soc.* **2013**, *135*, 17952−17957. (e) Zhang, P.; Zhang, L.; Wang, C.; Xue, S. F.; Lin, S. Y.; Tang, J. K. *J. Am. Chem. Soc.* **2014**, *136*, 4484−4487.

(4) Blagg, R. J.; Ungur, L.; Tuna, F.; Speak, J.; Comar, P.; Collison, D.; Wernsdorfer, W.; McInnes, E. J. L.; Chibotaru, L. F.; Winpenny, R. E. P. *Nat. Chem.* **2013**, *5*, 673−678.

(5) Rinehart, J. D.; Long, J. R. *Chem. Sci.* **2011**, *2*, 2078−2085.

(6) (a) Guo, Y. N.; Xu, G. F.; Guo, Y.; Tang, J. K. *Dalton Trans.* **2011**, *40*, 9953−9963. (b) Zhang, P.; Guo, Y. N.; Tang, J. K. *Coord. Chem. Rev.* **2013**, *257*, 1728−1763.

(7) (a) Liu, J. L.; Chen, Y. C.; Zheng, Y. Z.; Lin, W. Q.; Ungur, L.; Wernsdorfer, W.; Chibotaru, L. F.; Tong, M. L. *Chem. Sci.* **2013**, *4*, 3310−3316. (b) Liu, J. L.; Wu, J. Y.; Chen, Y. C.; Mereacre, V.; Powell, A. K.; Ungur, L.; Chibotaru, L. F.; Chen, X. M.; Tong, M. L. *Angew. Chem., Int. Ed.* **2014**, *53*, 12966−12970.

(8) (a) Koo, B. H.; Lim, K. S.; Ryu, D. W.; Lee, W. R.; Koh, E. K.; Hong, C. S. *Chem. Commun.* **2012**, *48*, 2519−2521. (b) Le Roy, J. J.; Ungur, L.; Korobkov, I.; Chibotaru, L. F.; Murugesu, M. *J. Am. Chem. Soc.* **2014**, *136*, 8003−8010.

(9) (a) Layfield, R. A.; McDouall, J. J. W.; Sulway, S. A.; Tuna, F.; Collison, D.; Winpenny, R. E. P. *Chem.—Eur. J.* **2010**, *16*, 4442−4446. (b) Sulway, S. A.; Layfield, R. A.; Tuna, F.; Wernsdorfer, W.; Winpenny, R. E. P. *Chem. Commun.* **2012**, *48*, 1508−1510. (c) Tuna, F.; Smith, C. A.; Bodensteiner, M.; Ungur, L.; Chibotaru, L. F.; McInnes, E. J. L.; Winpenny, R. E. P.; Collison, D.; Layfield, R. A. *Angew. Chem., Int. Ed.* **2012**, *51*, 6976−6980.

(10) (a) Birmingham, J. M.; Wilkinson, G. *J. Am. Chem. Soc.* **1956**, *78*, 42−44. (b) Maginn, R. E.; Manastyrskyj, S.; Dubeck, M. *J. Am. Chem. Soc.* **1963**, *85*, 672−676.

(11) (a) Zabrodsky, H.; Peleg, S.; Avnir, D. *J. Am. Chem. Soc.* **1992**, *114*, 7843−7851. (b) Pinsky, M.; Avnir, D. *Inorg. Chem.* **1998**, *37*, 5575−5582.

(12) Guo, Y. N.; Xu, G. F.; Guo, Y.; Tang, J. K. *Dalton Trans.* **2011**, *40*, 9953−9963.

(13) (a) Rinehart, J. D.; Meihaus, K. R.; Long, J. R. *J. Am. Chem. Soc.* **2010**, *132*, 7572−7573. (b) Meihaus, K. R.; Rinehart, J. D.; Long, J. R. *Inorg. Chem.* **2011**, *50*, 8484−8489.

(14) Singh, S. K.; Gupta, T.; Rajaraman, G. *Inorg. Chem.* **2014**, *53*, 10835−10845.

(15) Zheng, Y.-Z.; Zheng, Z.; Chen, X.-M. *Coord. Chem. Rev.* **2014**, *258*−*259*, 1−15.

DOI: 10.1021/acs.inorgchem.5b00213
Inorg. Chem. 2015, 54, 4588−4590